

International Conference on Technologies and Materials for Renewable Energy, Environment and Sustainability, TMREES15

SVPWM performance of PMSM variable speed and impact of diagnosis sensors faults

Lachtar Salah^a, Bahi Tahar^b

^a *Unité de Recherche en Energies Renouvelables en Milieu Saharien*

Centre de développement des énergies renouvelables, CDER, 01000, Adrar, Algérie,

^a *Department of Electrical Engineering, Annaba university BP12, 23000, Annaba, Algeria*

^b *Department of Electrical Engineering, Annaba university BP12, 23000, Annaba, Algeria*

Abstract

In this paper, the performances of a permanent magnet synchronous motor and impact of the control method on the diagnosis strategy are presented. First, permanent magnet synchronous motor and two level three phase inverter with space vector PWM strategy is developed. The PMSM speed is controlled by sliding mode control. A comparative study between standard and symmetric SVPWM methods is used. Latest part is devoted to treat fault detection on the sensors by a state estimation method. In our case, the sensors to monitor are those of the phase currents. Simulation results in superposition for both SVPWM methods have been compared, and fault detection diagnoses are presented.

© 2015 The Authors. Published by Elsevier Ltd. This is an open access article under the CC BY-NC-ND license (<http://creativecommons.org/licenses/by-nc-nd/4.0/>).

Peer-review under responsibility of the Euro-Mediterranean Institute for Sustainable Development (EUMISD)

Keywords: PMSM, SVPWM, two level inverter, variable structure control (VSC), currents sensors;

1. Introduction

Permanent magnet synchronous motor (PMSM) has received widespread acceptance, mainly in high performance of its applications for renewable energy generator or industrial servo applications of accurate speed and position control. This is due to some of its excellent features such as super power density, high torque to current ratio, fast response and low noise [1,2]. Strategies are defined at the early stages of concept so as to facilitate the control and fault detection. However, the synchronous motor fed by two present methods, especially for applications of great power performances at low speed operation without position or speed sensor. For the phase currents, we provide a simple approach for diagnosis and fault detection based on processing signals issued from the currents sensors [3,4]. Indeed, various methods have been applied in recent decades, and the implementation of the observers is often used

to reconstruct the rotor position from the phase currents and voltages [5]. For this, the theory of sliding mode [6], come from the variable structure control (VSC) family has been used for the PMSM driving control (see Fig. 1). The article content, present initially the synthesis of the speed controller in sliding mode applied to a PMSM control [7]. We will start in the first time, to present the elements modeling of the synchronous motor followed by direct torque control. The machine and the inverter which feeds it are briefly described. A complete model approach is simulated and results for the considered machine are presented to evaluate the performance of a proposal control when it is fed with a two level inverter with space vector PWM strategy [8].

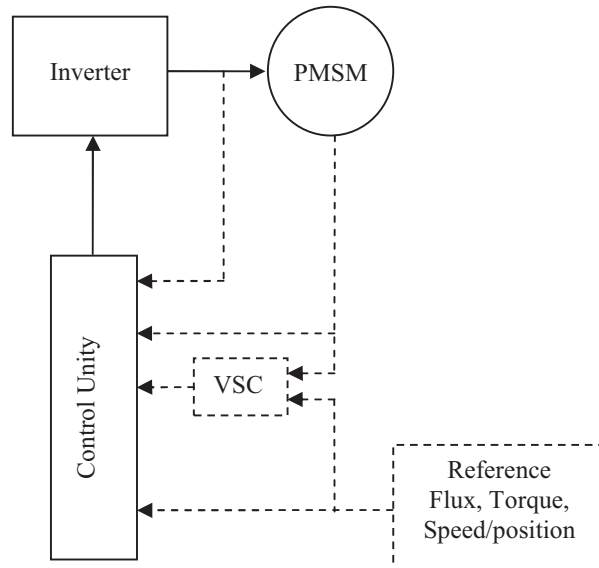


Fig. 1. PMSM control scheme

2. Model of the PMSM drive system

Synchronous permanent magnet motor (PMSM) comprises a three-phase stator winding represented by the three axes (a, b, c) phase shifted relative to each other by 120° electric, and permanent magnets rotor ensuring its excitation. The control of PMSM can be done by connecting to the inverter fed by a constant DC voltage source. The voltages of the inverters allow the imposition to the machine stator windings the amplitude and frequency voltages adjustable and acting on the control of the inverter switches. The PMSM drive is highly dependent on the sensors availability. When the sensor reading lost, the standard control stops or significantly disrupted. The electric drive is equipped with three currents sensors (due to safety requirements). The speed is generally estimated and followed by a sliding mode controller. The model of the PMSM is represented by the following equations system:

$$\begin{cases} \dot{X} = AX + BU \\ Y = CX \end{cases} \quad (1)$$

In a two level three-phase inverter, the voltage measured between the output of each inverter leg and the neutral point can have two values, U_c or V_{k0} with:

$$V_{k0} = S_k \cdot U_c \quad (2)$$

Where, S_k the signal controls k connects, and U_c the voltage rectified at the inverter input.

The operation can be described as follow:

- $S_k = 1$: switch top is closed and switch bottom is open.
- $S_k = 0$: switch top is opened and switch bottom is closed.

Admitting that the point (n) is a neutral, the neutral line voltage can be evaluated as follow:

$$\begin{bmatrix} V_{1n} \\ V_{2n} \\ V_{3n} \end{bmatrix} = \frac{1}{3} U_c \begin{bmatrix} 2S_1 & -S_2 & -S_3 \\ -S_1 & 2S_2 & -S_3 \\ -S_1 & -S_2 & 2S_3 \end{bmatrix} \quad (3)$$

The application of the Clarke frame allows the establishment of $(1, 2, 3 \rightarrow \alpha \beta)$.

$$\begin{bmatrix} V_\alpha \\ V_\beta \end{bmatrix} = U_c \begin{bmatrix} S_1 & -\frac{1}{2}S_2 & -\frac{1}{2}S_3 \\ 0 & \sqrt{\frac{1}{2}}S_2 & -\sqrt{\frac{1}{2}}S_3 \end{bmatrix} \quad (4)$$

Therefore, the space voltage vector \bar{V}_s is writing as follow:

$$\bar{V}_s = V_\alpha + jV_\beta = \sqrt{\frac{2}{3}} (V_{1n} + V_{2n}e^{j\frac{2\pi}{3}} + V_{3n}e^{-j\frac{2\pi}{3}}) \quad (5)$$

In this work, the flux estimate is carried out by the integration of the stator voltage. The selection of the voltage vector depends on the position of stator flux.

$$\frac{d}{dt} \begin{bmatrix} \hat{\phi}_{\alpha s} \\ \hat{\phi}_{\beta s} \end{bmatrix} = \begin{bmatrix} V_{\alpha s} & -R_s I_{\alpha s} \\ V_{\beta s} & -R_s I_{\beta s} \end{bmatrix} \quad (6)$$

$$\bar{\phi}_s = \sqrt{\hat{\phi}_{\alpha s}^2 + \hat{\phi}_{\beta s}^2} \quad (7)$$

The space where the flux vector $\bar{\phi}_s$ located is determined from the components $\hat{\phi}_{\alpha s}$ and $\hat{\phi}_{\beta s}$.

The electromagnetic torque is given by:

$$\hat{T}_e = p.(\hat{\phi}_{\alpha s} I_{\beta s} - \hat{\phi}_{\beta s} I_{\alpha s}) \quad (8)$$

The value recalculated of electromagnetic torque is compared with that of its reference. The output of hysteresis bands is a function of the error value. $k_c = 1$ torque grows, $k_c = 0$ torque decrease and $k_c = -1$ stable torque. In a similar way, measured flux will be compared with flux of reference, but by using a hysteresis bands on two levels. $k_\varphi = 1$: flux grows; $k_\varphi = 0$: flux decrease. The output of the hysteresis bands must indicate the direction of module evolution of $\bar{\phi}_s$, in order to select the corresponding voltage vector.

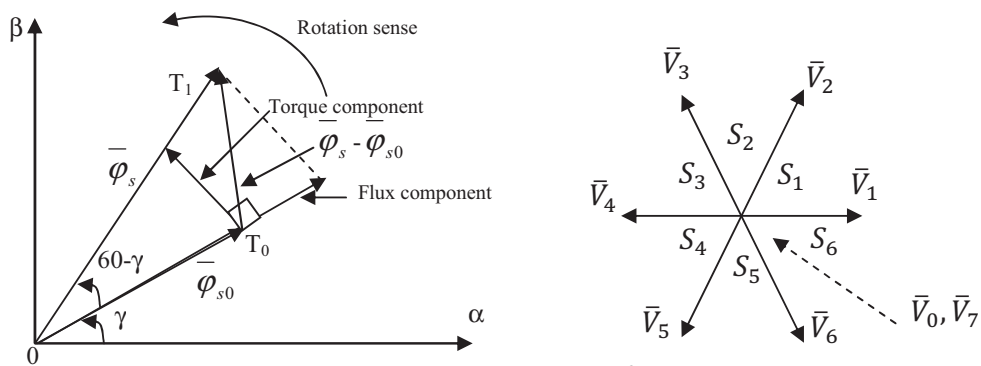


Fig. 2. Evolution of the flux vector in the plan (α, β) divided on six sectors

2.1. Switching sequences table

The table of switching proposed by the technique of the Direct Torque Control (DTC) is as follows:

Table 1. Switching sequences							
Sector (S)		1	2	3	4	5	6
$k_{\varphi=1}$	$k_c=1$	110	010	011	001	101	100
	$k_c=0$	111	000	111	000	111	000
	$k_c=-1$	101	100	110	010	011	001
$k_{\varphi=0}$	$k_c=1$	010	011	001	101	100	110
	$k_c=0$	000	111	000	111	000	111
	$k_c=-1$	001	101	100	110	010	011

With DTC, the stator flux and torque can be controlled simultaneously [9]. The control of the torque is ensured by a switching between the zero sequence states (the voltages applied at the machine poles are null, stator flux is fixed) and the active states (the machine is supplied, stator flux evolves) [10]. An increase in the reference torque led to an acceleration of flux, so, an increase in the sliding and torque \hat{T}_e . Conversely, minimizing in the reference torque involves a deceleration of stator flux, so minimizing in the sliding and torque \hat{T}_e .

3. The two level inverter modeling and control

The topology of a two level voltage inverter is shown in figure 3. Because of the constraint that the input lines must never be shorted and the output current must always be continuous a voltage source inverter can assume only eight distinct sequences. These sequences are shown on the table 2. Six out of these eight sequences produce a non-zero output voltage and are known as non-zero switching states and the remaining two sequences produce zero output voltage and are known as zero switching states.

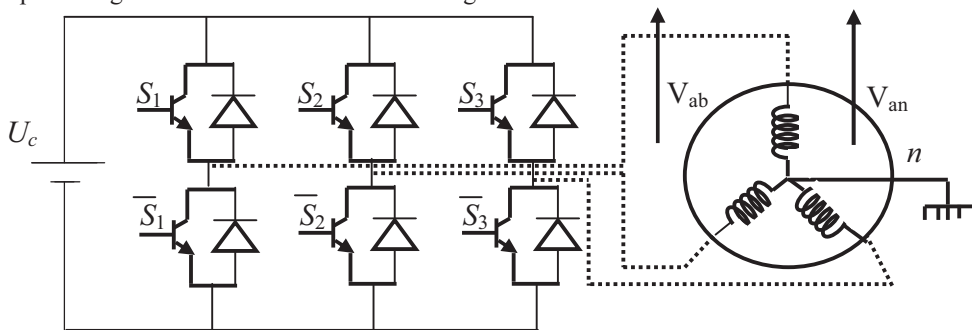


Fig. 3. Two level-inverter structure

3.1. Eight state voltages table

Table 2. Eight state voltages sequence

Voltage	V_0	V_1	V_2	V_3	V_4	V_5	V_6	V_7
Switch	$\bar{S}_1 \bar{S}_2 \bar{S}_3$	$S_1 \bar{S}_2 \bar{S}_3$	$S_1 S_2 \bar{S}_3$	$\bar{S}_1 S_2 \bar{S}_3$	$\bar{S}_1 S_2 S_3$	$\bar{S}_1 \bar{S}_2 S_3$	$S_1 \bar{S}_2 S_3$	$S_1 S_2 S_3$

3.2. Standard sequence SVPWM analysis

This method involves applying all existing vectors from V_0 to V_7 in the table 2. These vectors are characterized by the presence of the zero-sequence (see Fig. 4).

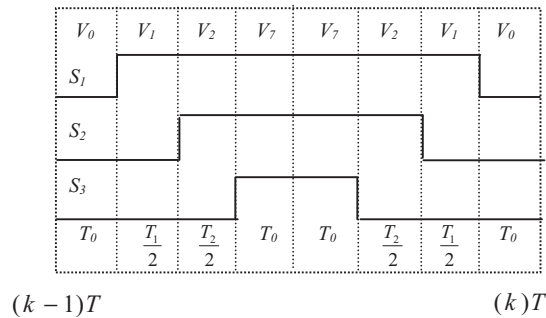


Fig. 4. Phase gating signals in SVPWM

$$T_0 = \frac{T - (T_1 + T_2)}{4}, \quad T_1 = \frac{(\sqrt{6}V_{s\alpha} - \sqrt{2}V_{s\beta})}{2.U_c} T, \quad T_2 = \frac{\sqrt{2}V_{s\beta}}{U_c} T \quad (9)$$

3.3. Symmetric sequence SVPWM analysis

Figure 5 shows specific topology for inverters where the three phase currents are not balanced. Thus, the sum of the phase currents is not zero and that is called the zero sequence current. By using only one zero vector, V_0 or V_7 within a given sector one of the legs does not have to be switched at all.

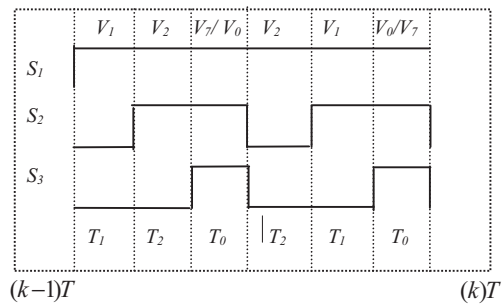


Fig. 5. Choice zero sequence of phase gating signals in SVPWM

Since the choice of the zero sequence voltages is based on the desired output voltage vector and the phase and magnitude of the current are determined by the load. The choice of zero vectors in sector 1 is determined using the follow algorithm.

$$\begin{cases} \text{if } |I_a| > |I_c| \text{ then } T_0 \leftrightarrow V_7 \\ \text{if } |I_a| < |I_c| \text{ then } T_0 \leftrightarrow V_0 \end{cases} \quad (10)$$

3.4. Simulation results two level inverter with SVPWM strategy

Taking into account the phase current form for both methods, the symmetric method is the most effective for the control of the three-phase inverter. If we compare the symmetric method against the other standard, the standard method has a very high ripple current, (see Fig. 6).

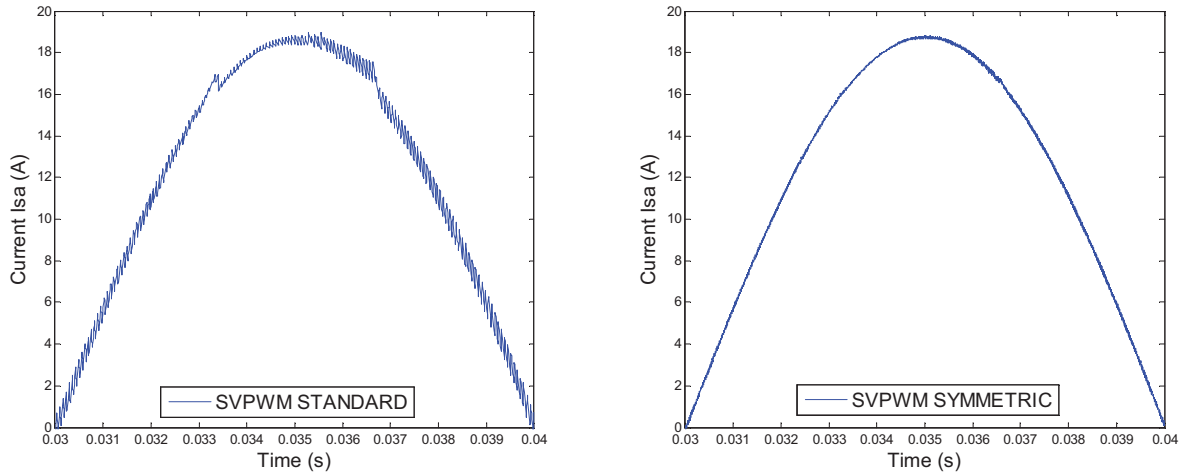


Fig. 6. Signals current phase "A" for both SVPWM methods

4. Speed control process

The algorithms of the conventional control using controllers with proportional, integral and derivative used to precisely control undisturbed linear process with constant parameters. When the ordered part is subject to disturbances and variations of the system parameters, an adaptive self solution, which by adjustment of regulatory parameters, allows keeping the performance set in advance in the presence of disturbances and changes in parameters. This solution often has the disadvantage of requiring complex implementation. It is possible to record a simpler solution, using a particular class of control systems, called "systems with variable structures control (VSC)", these systems implement in an important works since many years ago [11]. The recent interest in this technique of control is mainly due to the availability of more efficient electronic components and highly developed microprocessors

4.1. Synthesis of the control law

The synthesis variable structure law for the synchronous motor speed control is considered starting from the mechanical equation as:

$$J \frac{d\Omega}{dt} + f \Omega = T_e - T_l \quad (11)$$

The variable structure control modeling leads to differential equation with the following form:

$$\dot{x} = f(t, x) \quad (12)$$

The condition for obtaining the sliding mode is:

$$S(x) \dot{S}(x) < 0 \quad (13)$$

4.2. Smooth control law

High frequency oscillations appearing on the response in discontinuous control law can be avoided by the smooth control law, replacing the function signs by the function continues close:

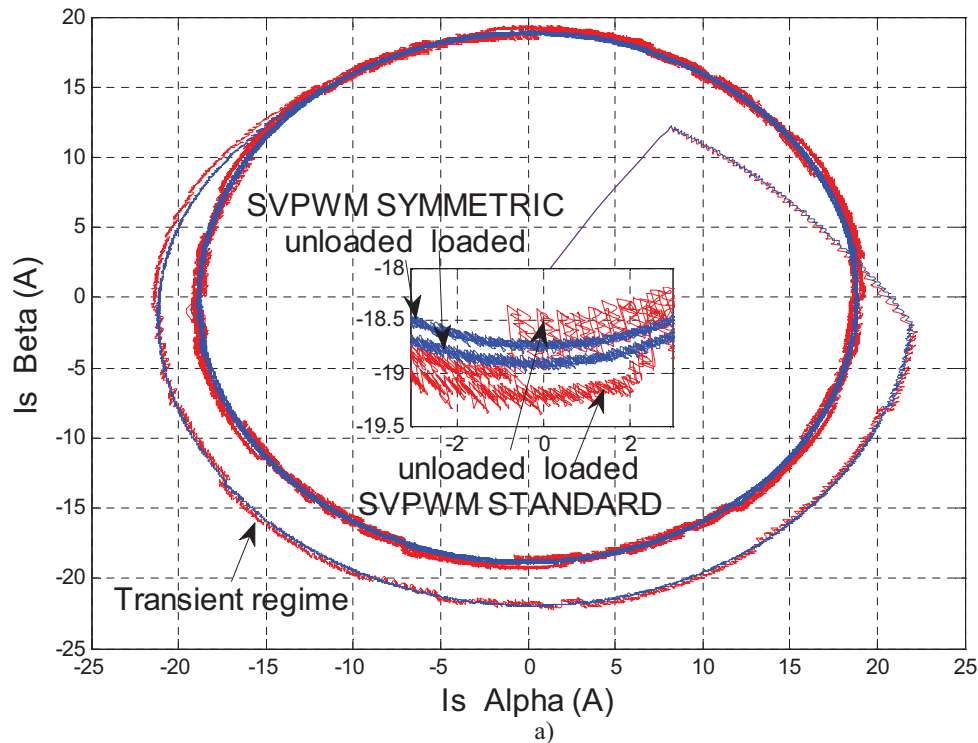
$$U = K \cdot \frac{S_{\Omega}}{|S_{\Omega}| + \delta} + \sigma \quad \delta = \delta_0 + |\rho| \quad (14)$$

$$\begin{cases} \text{if } -\varepsilon < S_{\Omega} < \varepsilon & \text{then } \rho = \rho_0 \\ \int S_{\Omega} dt; \quad \sigma = \sigma_0 \int S_{\Omega} dt \\ \text{if } \varepsilon < S_{\Omega} < -\varepsilon & \text{then } \rho = 0; \quad \sigma = 0 \end{cases} \quad (15)$$

In general, the δ , σ and ε are determined by trial and error and they are selected in order to define the control performances such as: rapidity, precision and robustness by the numeric simulation.

4.3. Simulation results of speed control

We tested the operation of the PMSM supplied by a two level inverter with both SVPWM methods. The motor is loaded with a torque of 5 Nm at $t=0.05$ s. the obtained superposition results of current, speed and torque for the two cases of power supplies. Noting that the currents in the (α, β) plane are less oscillatory and more stable with symmetric method compared to other standard method (see Fig.7a). Same cases for the speed (Fig.7b) and the torque (Fig.7c) have a faster response in transient regime.



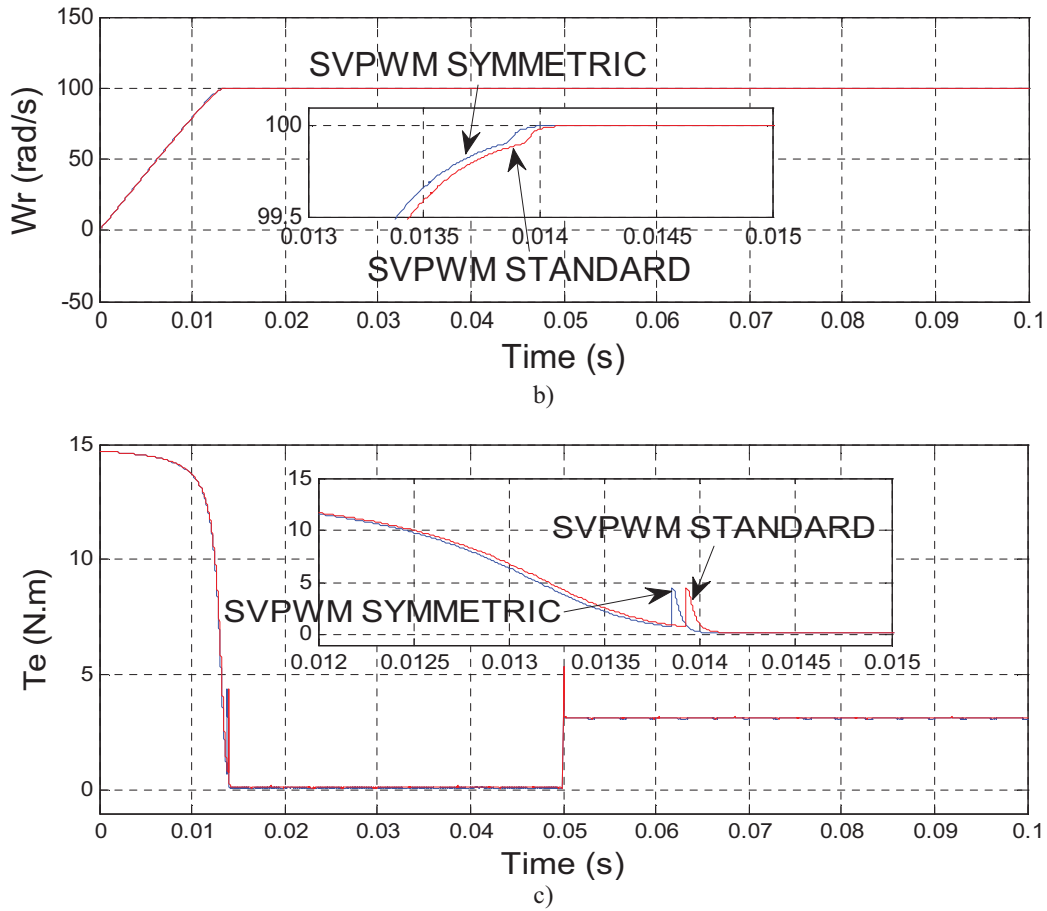


Fig. 7 PMSM fed by two level-inverter with and without zero state voltages

5. Currents sensor diagnosis

Given the electrical model of the PMSM, phase currents can be expressed as a function of the tension, position and speed. The estimated speed is used with the reference voltages to estimate three-phase currents ($\hat{i}_a, \hat{i}_b, \hat{i}_c$). An adaptive control by the reference model is used with a state feedback [12,13]. The aim is to compare a closed loop control with variable settings to change the adjustable model with a reference model.

5.1. Observer model of currents

The reference model determines desired states (phase currents) and the adjustable model generates the estimated states [14, 15, 16, 17]. The PMSM with the currents in the rotating frame as state variable considered:

$$\dot{x} = Ax + Bu \quad (16)$$

$$\begin{bmatrix} \dot{x}_1 \\ \dot{x}_2 \end{bmatrix} = \begin{bmatrix} -\frac{R_s}{L_d} & \frac{L_q}{L_d} w \\ -\frac{L_d}{L_q} w & -\frac{R_s}{L_q} \end{bmatrix} \begin{bmatrix} x_1 \\ x_2 \end{bmatrix} + \begin{bmatrix} \frac{1}{L_d} & 0 \\ 0 & \frac{1}{L_q} \end{bmatrix} \begin{bmatrix} u_d \\ u_q \end{bmatrix} \quad (17)$$

$$x = [x_1, x_2] = \left[i_d + \frac{\phi}{L_d}, i_q \right] \quad (18)$$

$$u = [u_d, u_q] = \left[u_d + \frac{R_s}{L_d} \phi, u_q \right] \quad (19)$$

The state feedback control law is written: $U = -Kx$ where $K = [k_1, k_2]$ is the state feedback gain. The currents can therefore be estimated by:

$$\dot{\hat{x}} = (A - BK)\hat{x} \quad (20)$$

5.2. Stability analysis

For a non-linear system, the existence of a Lyapunov function condition is sufficient to ensure the asymptotic stability. A Lyapunov function V is a positive definite function with its Lie derivative \dot{V} , which is defined negative. PMSM for a function Lyapunov candidate is:

$$V(x) = \frac{1}{2}(x_1^2 + x_2^2) \text{ avec } V(x) \geq 0 \quad (21)$$

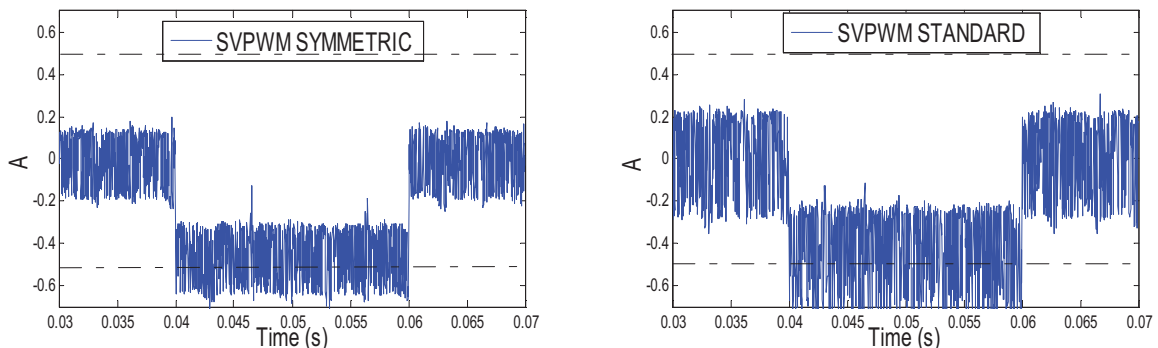
$$\dot{V} = x_1 \dot{x}_1 + x_2 \dot{x}_2$$

$$\dot{V} = -\frac{1}{L_d}(R_s + k_1)x_1^2 - \frac{1}{L_q}(R_s + k_2)x_2^2 + x_1 x_2 \left(-\frac{k_1 + L_d w}{L_q} - \frac{k_2 - L_q w}{L_d} \right) \quad (22)$$

Choosing K such as $k_1 = -L_d w, k_2 = L_q w$, the stability is ensured. Thus, by applying the reverse Park transformed and Concordia, the three-phase currents is estimated $[\hat{i}_a, \hat{i}_b, \hat{i}_c]$.

5.3. Simulation results

Validating the current sensor fault detection method is carried out using the same system described above. A fault of 15% of current amplitude is inserted during operation at the phase sensor A from $t = 0.04$ s to $t = 0.06$ s. Figure 8 shows the observer residues of currents for both methods (symmetric and standard SVPWM). The most important change is noticed in the residue A which indicates that the fault measurement affects the phase of the sensor A (Fig.8a). Changes in the other two residues (Fig.8b) and (Fig.8.c) are due to the mathematical relationship between the three phases (plan Park). From $t = 0.06$ s estimating current was strong against this variation. Thus, the current observer is both accurate transient than permanent regime. Important undesirable fluctuations and oscillations on the residues with the standard method (Fig.8 right) compared by symmetric method (Fig.8 left).



a)

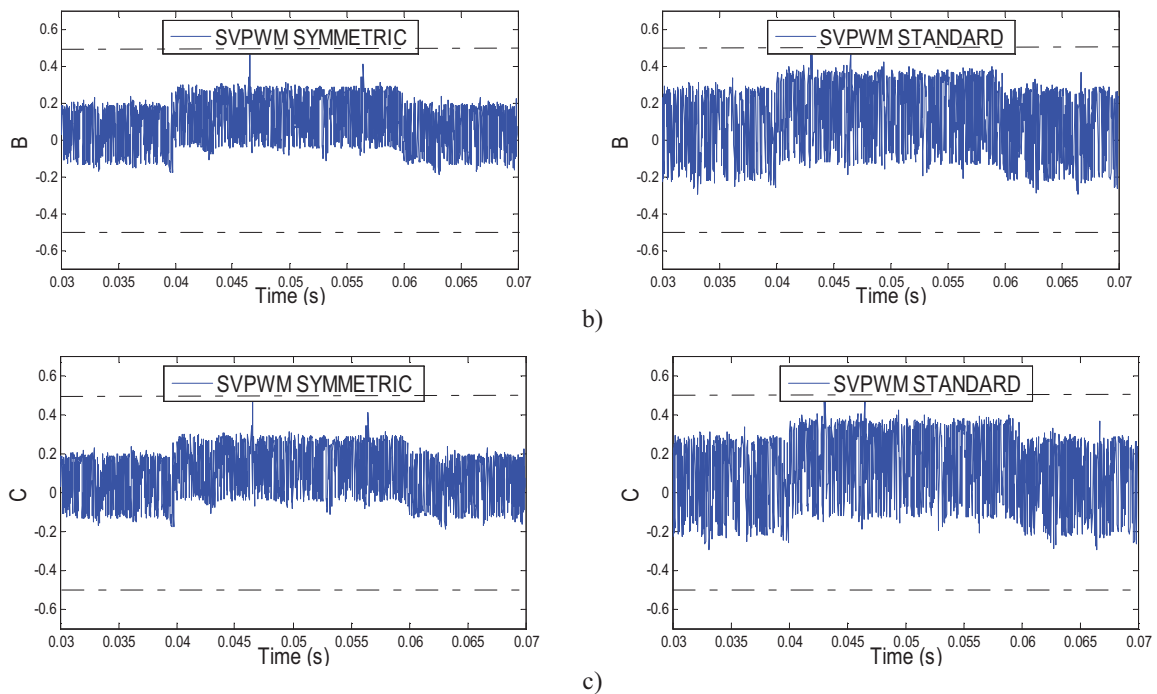


Fig. 8. Residues currents sensors

6. Conclusion

In this paper, we presented the PMSM fed by three phase inverter. Specifically we are interested to show the system output signals for two methods (Standard and Symmetric SVPWM) which are compared to see the both methods performances. This system supplied by faults detection structure sensors currents. The fault detection based on an adaptive observer of currents. The decision is made easy as the calculating residues demonstrate its practical results and efficiency in a faults current sensors case.

If we compare the symmetric method compared to the standard method, we find that the both methods have the same total number of switches (6 switching), and are evenly distributed (2 switches per leg) but the standard method has a high ripple current (Fig.7a), a slow response speed (Fig.7b) and torque (Fig.7c), hence the choice of symmetric method compared to the standard method.

The detection threshold is shown in dotted lines on each residue (see Fig.8). Thus, the current observer is generally accurate transient than permanent regime. Finally, setting a threshold of 0.5 for each phase, the logic signals are obtained which allowed activating the detection (Fig.8a). This bias value is chosen, because under this latter (0.5), the impact of the fault on sensor control is negligible (Fig.8b) and (Fig.8c).

References

- [1] Fayed FM, El-Sousy. HybridHN-Based Wavelet-Neural-Network Tracking Control for Permanent-Magnet Synchronous Motor Servo Drives. IEEE Trans- actions in industrial Electronics 2010; 57(9):33–9.
- [2] Ghafari-Kashani AR, Faiz J, Yazdanpanah. MJ. Integration of non-linear H1 and sliding mode control techniques for motion control of a permanent magnet synchronous motor. IET Electronics Power 2010;4(4):267–80.
- [3] Y.A.Ibrahim Mohamed, E.F.El-Saadany. A current control scheme with an adaptive internal model for torque ripple minimization and robust current regulation in PMSM drive systems, IEEE Trans. Energy Convers. 23(2008) 92–100.
- [4] Nuno M. A. Freire, Jorge Estima, A. J. M. Cardoso. New Approach for Current Sensor Fault Diagnosis in PMSG Drives for Wind Energy Conversion Systems. IEEE Transactions on Industry Applications; Mar 2014.

- [5] Chang S-H, Chen P-Y, Ting Y-H, Hung S-W. Robust current control-based sliding mode control with simple uncertainties estimation in permanent magnet synchronous motor drive systems. *IET Electronics Power* 2010;4(6): 441–50.
- [6] Ghafari-Kashani AR, Faiz J, Yazdanpanah. MJ. Integration of non-linear H1 and sliding mode control techniques for motion control of a permanent magnet synchronous motor. *IET Electronics Power* 2010; 4(4):267–80.
- [7] K. Kang, J. Kim, K. B. Hwang, and K. H. Kim. Sensorless control of PMSM in high speed range with iterative sliding mode observer. in *Conf. Rec. IEEE APEC*, vol. 2, pp. 1111-1116, 2004.
- [8] Urresty JC, Riba JR, Delgado M, Romeral L. Detection of demagnetization faults in surface-mounted permanent magnet synchronous motors by means of the zero-sequence voltage component. *IEEE Trans Energy Convers* 2012;27:42–51.
- [9] Pyrhonen. O, Niemela. M, Pyrhonen. J, Kaukonen. J. Excitation control of DTC controlled salient pole synchronous motor in field weakening range. In *International work shop on advanced motion control*; Coimbra;1998 AMC'98 p. 294–298.
- [10] N.M.Silva, A.P.Martins, A.S.Carvalho. Torque and Speed What if mode of have DTC-Controlled Induction Motor. *Proceedings of the 10th Mediterranean Conference on Control and Automation-MED 2002*, Lisbon, Portugal, July 9-12, 2002.
- [11] R. A. DeCarlo, S. H. Zak, G. P. Matthews. Variable structure control of nonlinear multivariable systems: A tutorial. *Proc. IEEE*, vol. 76, p. 212-232, 1988.
- [12] Lee. B, Jeon. N, Lee. H. Current sensor fault detection and isolation of the driving motor for an in-wheel motor drive vehicle. *International conference on Control, Automation and Systems (ICCAS)*, vol., no., p.486, 491, 26-29 Oct. 2011.
- [13] Najafabadi. T, Salmasi. F, Jabejdar-Maralani. P. Detection and Isolation of Speed-, DC-Link Voltage and Current-Sensor Faults Based on an Adaptive Observer in Induction-Motor Drives. *IEEE Transactions on Industrial Electronics*, vol. 58, no. 5, 2011.
- [14] Akrad. A, Hilaiet. M, Diallo. D. Design of a Fault-Tolerant Controller Based on Observers for a PMSM Drive. *Industrial Electronics, IEEE Transactions on*, vol.58, n° 4, p.1416-1427, April 2011.
- [15] Rothenhagen. K, F. W. Fuchs. Current Sensor Fault Detection, Isolation, and Reconfiguration for Doubly Fed Induction Generators. *Industrial Electronics, IEEE Transactions on*, vol.56, no.10, pp.4239- 4245, Oct 2009.
- [16] Foo, G.H.B. ; Xinan Zhang ; Vilathgamuwa, D.M.; " A Sensor Fault Detection and Isolation Method in Interior Permanent-Magnet Synchronous Motor Drives Based on an Extended Kalman Filter," *IEEE Transactions on Industrial Electronics*, vol.60, no.8, pp.3485- 3495, 2013
- [17] Nuno M. A. Freire, Jorge Estima, A. J. M. Cardoso;"New Approach for Current Sensor Fault Diagnosis in PMSG Drives for Wind EnergyConversion Systems" *IEEE Transactions on Industry Applications* , Mar 2014